

# MULTI-SCENARIO PREVIEW AND DYNAMIC VERIFICATION OF POWER GRID OPERATION BEHAVIOR BASED ON VIRTUAL REALITY TECHNOLOGY

Tiancheng WEN<sup>1\*</sup>, Chao HU<sup>2</sup>, Zhangguo CHEN<sup>2</sup>, Weiwei PENG<sup>2</sup>

*This paper addresses the complexity of power grid operation behavior by developing a multi-scenario preview and dynamic verification method leveraging virtual reality (VR) technology. The method integrates real-time positioning data, operation ticket information, and environmental variables to construct an immersive 3D virtual scene that closely replicates actual grid equipment and conditions. Within this virtual environment, the behavior and responses of grid operators under various fault scenarios are simulated, enabling early risk identification and assessment. Dynamic verification algorithms are applied to validate operational behavior in real time, providing data-driven decision support for dispatchers. Experimental results demonstrate that the VR-based approach achieves a success rate of at least 85% in scenarios including line faults, equipment faults, load overload, and frequency fluctuations, with an average response time of 16.5 seconds and a behavior simulation recognition accuracy of about 90%. Additionally, the dynamic verification algorithm recorded a MAE (Mean Absolute Error) of 0.03 and an MSE (Mean Squared Error) of 0.002 within 60 seconds. These findings highlight the innovative integration of immersive VR and dynamic verification techniques, offering a robust tool for enhancing the safety and reliability of power grid operations.*

**Keywords:** Virtual Reality Technology; Power Grid Operation; Multi-Scenario Preview; Dynamic Verification; Risk Identification

## 1. Introduction

The power grid is the most important part of energy circulation in modern society. The complexity of its operation behavior is increasing. Under changing environments and various operating conditions, the safety and stability of power grid operation are very important [1,2]. The application of VR technology began to receive attention, simulating grid operations in a realistic virtual environment, and conducting behavior rehearsals and risk verification [3,4]. Immersive virtual reality technology provides more intuitive decision support for power grid dispatching and a highly interactive training platform for power grid operators.

Grid operations involve complex multi-scenario environments, and operators need to respond quickly to emergencies in different situations. Traditional

---

<sup>1</sup> \* Foshan Power Supply Bureau of Guangdong Power Grid Co., Ltd., Foshan, Guangdong, 528000, China, corresponding author: Tiancheng Wen, 3584074767@qq.com

<sup>2</sup> Nanjing NARI Information and Communication Technology Co., Ltd, Nanjing, Jiangsu, 211100, China

rehearsal and verification methods rely on static simulation and single-scenario training, which cannot reflect the dynamic changes in grid operation [5,6]. Static simulation provides certain operational guidance but lacks flexibility and adaptability in complex grid environments with sudden failures, equipment performance fluctuations, and other changes [7,8]. Reaction speed and judgment in the face of emergencies are also important conditions. Current training methods cannot effectively improve operators' adaptability in diverse environments [9,10].

In the current multi-scenario operational behavior rehearsal, dynamic changes in the environment are rarely taken into account [11,12]. Grid equipment, environmental variables, and operation ticket information are provided to operators in the form of static data, and the training process lacks interactivity [13,14]. A single scenario simulation cannot accurately reproduce the complex variables and situations that may be encountered during actual grid operation. It is difficult to identify potential operational risks, and potential problems cannot be discovered in advance.

Traditional verification methods rarely consider the real-time interaction between the operator's behavioral response and environmental changes. They rely on the verification of operating procedures and the monitoring of equipment status and cannot provide comprehensive feedback and correction of operating behavior [15,16]. The verification algorithms in the systems on the market mostly rely on offline analysis and lack real-time verification and feedback of operator behavior and environmental changes, resulting in the failure to timely discover and deal with potential risks [17,18]. The accuracy and safety of power grid dispatch are easily overlooked in the case of drastic environmental changes. A targeted and dynamic adjustment mechanism is needed to address the shortcomings of traditional methods in efficiently dealing with complex power grid problems [19,20].

This paper uses virtual reality technology to break through the limitations of current power grid operation behavior preview and verification and constructs a more accurate and dynamic simulation method. It can build realistic 3D virtual grid scenes, integrate real-time data and operation ticket information, and conduct real simulated grid operations in a variety of complex environments. This innovation can improve the visualization and interactivity of the operator's decision-making process. The timely feedback mechanism allows operators to intuitively evaluate the risks under different operating conditions in the virtual environment and optimize the decision path. The uniqueness of the research lies in that it not only simulates the standard operating procedures, but also reflects the impact of equipment status, environmental changes and emergencies on operating behavior. Using dynamic verification methods, according to the changes in the power grid operating status and environmental variables, the operating rules and verification processes are automatically adjusted to conduct real-time risk prediction and assessment. This improves the flexibility of power grid dispatching, allowing operators to respond

quickly when faced with complex situations and reduce potential risks. The fusion of environmental variables and real-time data is introduced into the simulation, and each rehearsal is highly consistent with the actual operation scenario, which improves the prediction accuracy of the operation behavior; this innovative combination method provides a new decision support platform for power grid dispatching, promoting the intelligence and precision of power grid operation.

## 2. Related Work

Many researchers have studied power grid operation behavior through drills and simulations, focusing on decision-making, risk identification, and operational path verification to enhance safety and accuracy. Some proposed simulation-based methods to model operator responses in emergencies [21,22]. Zhao examined dynamic state estimation in both synchronous motor-dominated and power-electronics-based systems, outlining future directions for next-generation energy management [23]. Others employed multi-scenario simulation algorithms to improve risk prediction during operations [24,25]. Lv introduced an online reliability assessment for cyber-physical systems using machine learning, spatiotemporal correlation detection, and intelligent control, enabling defenders in distributed control to allocate defense resources adaptively [26]. However, these approaches often address only specific scenarios and rely on static simulations, lacking real-time adaptation to dynamic environments.

To tackle dynamic adaptability, recent work has explored VR technology [27,28]. Its immersive nature offers intuitive, dynamic training and decision support. Integrating VR with real-time data streams has enabled virtual environments for multi-dimensional evaluation of operator behavior [29,30]. Awal M A' s unified virtual oscillation controller provides a seamless framework for grid-forming and grid-following converters, demonstrating superior fault ride-through and mode-switching without phase-locked loop issues [31]. Other studies combined virtual simulation with AI for multi-scenario operation optimization and risk assessment, yielding promising results [32,33]. Omitaomu O A' s survey highlighted AI' s role in smart grids but noted persistent challenges in load forecasting, stability assessment, fault detection, and security, calling for further research to boost grid resilience [34]. Yet existing methods still inadequately capture the operational complexity and real-time dynamics of actual grid environments. This paper addresses these gaps by integrating VR with equipment data, real-time environmental inputs, and dynamic verification algorithms, proposing a multi-scenario, multi-variable adaptive dynamic preview and verification method.

### 3. Methods

#### 3.1 3D Virtual Scene Construction and Environment Modeling

##### 3.1.1 Construction of three-dimensional model of power grid equipment

The 3D modeling of power grid equipment accurately reflects the VR operational environment. Laser scanning and photogrammetry extract equipment features to generate precise digital models, incorporating material, dimensions, and appearance to faithfully represent electrical components, wiring, and spatial layout. Customized workflows are developed for different equipment types (e.g., transformers, switches, circuit breakers), aided by CAD(Computer-Aided Design)[35 - 36] and BIM tools to enhance accuracy.

For complex equipment, geometric modeling is combined with texture mapping to ensure correct proportions and realistic surface details. Parametric modeling is used, defining multiple parameters aligned with real-world dimensions to enable scalability and reusability of each model. The formula is as follows:

$$V = \int_D f(x, y, z) dx dy dz \quad (1)$$

V represents the three-dimensional volume of the device,  $f(x, y, z)$  is the geometric shape function of the device surface, and D is the spatial area where the device is located; the formula accurately calculates the device model so that the device size in the model construction strictly meets the actual requirements.

Table 1

Output format of power grid equipment modeling			
Equipment Type	Modeling Technique	Input Data	Output Model Format
Transformer	Laser Scanning + Photogrammetry	Laser scanning point cloud data, photographic images	.obj, .fbx
Circuit Breaker	Laser Scanning + CAD Design	CAD drawings, electrical wiring diagrams	.dwg, .dxf
Switchgear	3D Modeling Software (AutoCAD)	Equipment dimensions, structural blueprints	.stl, .obj
Cables and Accessories	Laser Scanning + Visual Modeling	Site environmental maps, actual cable data	.stl, .obj

##### 3.1.2 Environmental modeling and scene integration

The environmental modeling stage focuses on the spatial features of operating sites and reconstructing operational environments. Multi-view data acquisition—applied to substations, distribution networks, etc.—is integrated with GIS and topographic maps to build virtual models of terrain, buildings, and external factors like weather and lighting, enabling scene variations under different times and weather conditions.

Physical modeling simulates the effects of climate, lighting, wind speed, and other environmental factors. Light intensity is modeled via ray tracing, while wind, temperature, and humidity are simulated using fluid dynamics. The light variation model is:

$$I(x, y, t) = I_0 \cdot \left( \frac{r}{d(x, y)} \right)^2 \cdot e^{-\alpha \cdot t} \quad (2)$$

$I(x, y, t)$  represents the light intensity at the coordinate point at time  $t$ ,  $I_0$  is the initial light intensity,  $r$  is the radiation intensity of the light source,  $d(x, y)$  is the distance from the light source to the point  $(x, y)$ , and  $\alpha$  is the attenuation coefficient, which represents the absorption and scattering effects in the environment; The impact of wind speed on grid equipment uses the Navier-Stokes equation in fluid mechanics to simulate air flow and predict the force of wind speed on equipment. The simplified wind speed model can be expressed as:

$$\vec{F} = \rho \cdot \vec{v} \cdot (\vec{v} \cdot \nabla) \vec{v} \quad (3)$$

$\vec{F}$  is the wind force acting on the power grid equipment,  $\rho$  is the air density,  $\vec{v}$  is the wind speed vector, and  $\nabla$  is the gradient operator.

Fig. 1 shows the key modules of 3D virtual scene construction and environment modeling and their interrelationships.

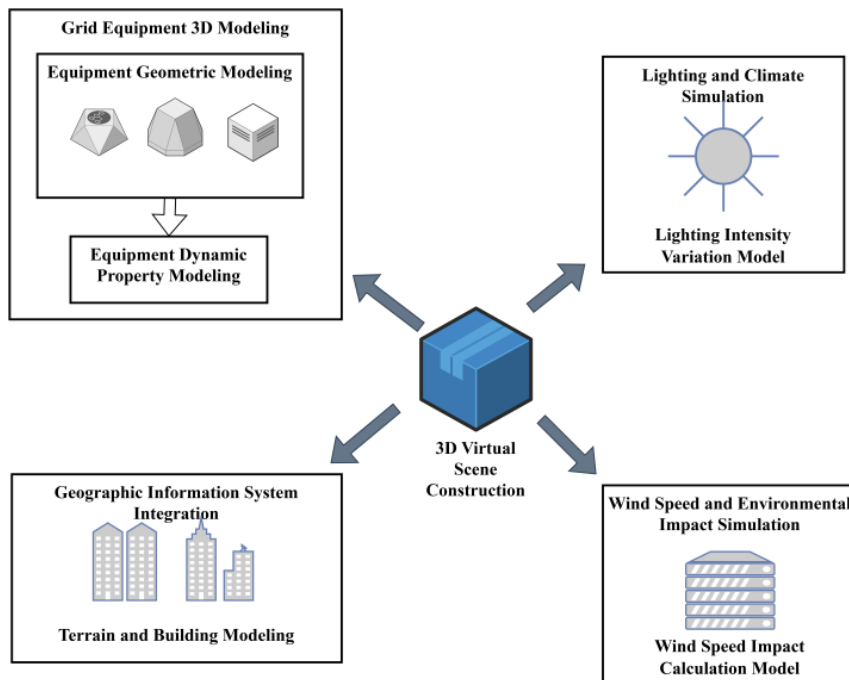


Fig. 1. Virtual scene construction and environment modeling

3D virtual scene construction, as a core node, relies on the modeling of equipment and environment; 3D modeling of power grid equipment consists of two parts:

equipment geometry modeling and equipment dynamic attribute modeling. The former ensures accurate restoration of the spatial structure of the equipment, while the latter enables the equipment to reflect its working status. Geographic Information System Integration provides geographic location data for power grid equipment, accurately locates terrain and buildings; Light and climate simulation simulates climate change in the external environment and adjusts the light intensity of the virtual scene; Wind speed and environmental impact simulation calculates the forces of environmental factors on power grid equipment, providing support for risk identification during operation. Each module works together to maintain the authenticity and dynamics of the virtual scene, supporting efficient rehearsal and risk detection of power grid operations.

### 3.2 Real-time Data Integration and Dynamic Scene Update

#### 3.2.1 Real-time data integration

Data integration enables dynamic updates of virtual scenes by timely collecting and processing operational field data. Equipment status, operation ticket information, and environmental variables are monitored in real time via sensors and monitoring systems. Sensors capture current, voltage, temperature, and other grid equipment states, transmitting them wirelessly to a data processing platform. GIS technology locates equipment and personnel, providing precise spatial information. This data is fused with operation ticket information using a multi-source data fusion algorithm. Sensor-derived current and voltage data undergo noise filtering and smoothing, accounting for sensor accuracy and sampling frequency. The noise-filtered value at time  $t$  is represented as:

$$x(t) = \frac{1}{n} \sum_{i=0}^{n-1} y(t-i) \quad (4)$$

$x(t)$  is the smoothed current or voltage data,  $y(t-i)$  is the original signal, and  $n$  is the window size, which represents the smoothing of the signal. Noise filtering eliminates mutations and errors in sensor data and provides more accurate grid equipment status data.

For the current change of the equipment, the Kalman filter algorithm can be used to estimate its true value and integrate it with the environmental data:

$$x_k = x_{k-1} + w_k \quad (5)$$

$x_k$  is the estimated equipment status,  $w_k$  is the process noise, and the sensor data is updated to provide an optimal estimate of the device status.

The Kalman filter algorithm parameters are configured as shown in Table 2. The process noise covariance  $Q$  is set to  $0.01 \cdot I$ , reflecting minor uncertainties in system states during grid operation; the measurement noise covariance  $R$  is set to  $0.1 \cdot I$ , corresponding to typical error ranges in sensor measurements. Both the state transition matrix  $A$  and observation matrix  $H$  are initialized at 1.0, based on the assumption of steady-state grid operation.

Table 2

Kalman filter parameter settings for real-time data optimization			
Parameter	Symbol	Value	Description
Process noise covariance	$Q$	$0.01 \cdot I$	Diagonal matrix, representing small system uncertainty due to grid dynamics.
Measurement noise covariance	$R$	$0.1 \cdot I$	Diagonal matrix, reflecting sensor noise
State transition matrix	$A$	1.0	Assumes constant state dynamics
Observation matrix	$H$	1.0	Direct measurement mapping
Initial state covariance	$P0$	$1.0 \cdot I$	Initial uncertainty in state estimation.

The initial state covariance  $P0$  is set to  $1.0 \cdot I$ , representing uncertainty in initial state estimation. These parameters were optimized through Monte Carlo simulation methods to minimize mean absolute error (MAE) and mean squared error (MSE). The parameter configuration reflects a design philosophy prioritizing confidence in the dynamic model (smaller  $Q$ ) over sensor measurements (larger  $R$ ), ensuring optimal filtering performance in grid operation data optimization.

### 3.2.2 Dynamic scene update

Combined with the VR engine, the real-time collected data can drive the update and interaction of the scene. Environmental variables, changes in equipment status, and the interactive behavior of operators can affect the presentation effect in the virtual scene. The changes in data must be accurately calculated and updated so that the virtual scene can reflect the on-site status in a timely manner.

The key to scene update is how to adjust various elements in the virtual environment according to dynamic data. During the operation, if a circuit breaker is operated, the switch state of the device can change accordingly; the state of the device in the virtual scene must also be updated synchronously with the actual state. The update can be described by the following formula:

$$S_{t+1} = f(S_t, \Delta t, \Delta p) \quad (6)$$

$S_{t+1}$  is the device state at time  $t + 1$ ,  $S_t$  is the device state at the current time,  $\Delta t$  is the time increment, and  $\Delta p$  is the state change. The state change of the device is related to the time and its operation state change.

For changes in environmental variables, factors such as lighting, temperature, and humidity in the virtual scene can also be affected by real-time data. The temperature sensor collects temperature changes in real time, and the temperature around the device in the virtual scene should also be adjusted accordingly. The following heat conduction model can be used to describe it:

$$\frac{\partial T}{\partial t} = \alpha \nabla^2 T + Q(x, t) \quad (7)$$

$T$  is the temperature field,  $\alpha$  is the thermal diffusion coefficient,  $\nabla^2 T$  is the second-order spatial derivative of temperature, and  $Q(x, t)$  is the distribution function of the heat source. Heat conduction describes the change of the temperature

field over time and the influence of the heat source on the temperature distribution; the virtual scene uses this model to dynamically simulate the thermal changes of the environment, so that the devices in the scene are synchronized with the environmental changes and enhance the immersion of VR.

### 3.3 Operational Behavior Simulation and Risk Identification

#### 3.3.1 Operation behavior simulation

The study uses virtual power grid equipment and environmental variables to accurately reproduce operators' task paths, decision-making processes, and reaction times. A task- and behavior-driven simulation framework models operator responses under varying conditions, where behavioral paths, steps, and execution are governed by virtual device states, environmental data, and control system feedback, yielding highly realistic results. Operators make decisions based on real-time equipment status and environmental information. Their state transitions and action selections are modeled via a Markov decision process: actions are chosen according to the current operator state, leading to a new state, with immediate feedback provided by a reward function:

$$Q(s_t, a_t) = r(s_t, a_t) + \gamma \max_{a_{t+1}} Q(s_{t+1}, a_{t+1}) \quad (8)$$

$Q(s_t, a_t)$  is the quality value of the current state and behavior, and  $\gamma$  is the discount factor, which reflects the impact of future rewards.

The reaction time of the operator to the operating condition is determined by the perceptual delay time and decision time. The reaction time can be expressed as:

$$T_r = T_p + T_d = \frac{K_1}{\sigma_1} + \frac{K_2}{\sigma_2} \quad (9)$$

$(K_1, K_2)$  are the operational complexity parameters of each task, and  $(\sigma_1, \sigma_2)$  are the efficiency factors of perception and decision-making in the task.

Table 3

Input variables for operation behavior simulation				
Variable Name	Description	Unit	Value Range	Set Value
$K_1$	Perception complexity parameter	Dimensionless	[0, 10]	5
$K_2$	Decision complexity parameter	Dimensionless	[0, 10]	3
$\sigma_1$	Perception phase efficiency factor	Seconds/Action	[0.1, 1.0]	0.6
$\sigma_2$	Decision phase efficiency factor	Seconds/Action	[0.1, 1.0]	0.4
$\gamma$	Discount factor	Dimensionless	[0, 1]	0.85

#### 3.3.2 Risk Identification

Risk identification analyzes the operator's behavior path and responses in simulation to detect potential risks—such as equipment failure, decision delays, or errors—by identifying anomalies in behavioral patterns. Each operation step is represented by a feature vector capturing behavior-related attributes. Deviations from normal behavior are quantified using a risk function based on path abnormality:

$$R(X) = \sum_{i=1}^n \lambda_i \cdot (x_i - \mu_i)^2 \quad (10)$$

$\lambda_i$  is the weight coefficient of the feature,  $\mu_i$  is the expected value of the feature  $x_i$ ; the risk function calculates the cumulative square error of the operation behavior deviation and quantifies the abnormal degree of the operator's behavior. If the value of the risk function exceeds the threshold, it means that the operation path has potential risks and needs further intervention or adjustment.

Risk identification also needs to consider environmental factors and dynamic changes in equipment status. Risks in power grid operations come not only from operator decision errors, but also from external factors such as equipment failures and environmental changes. A risk identification method based on state estimation is introduced in behavior identification. Real-time monitoring of equipment status and environmental variables, combined with operator behavior data, enables multi-dimensional risk assessment; the correlation between equipment abnormality and operator behavior can be evaluated using the following formula:

$$R_{\text{total}}(t) = \alpha \cdot R_{\text{op}}(t) + \beta \cdot R_{\text{env}}(t) + \gamma \cdot R_{\text{equip}}(t) \quad (11)$$

$R_{\text{total}}(t)$  is the risk of the operation behavior,  $R_{\text{env}}(t)$  is the risk caused by environmental factors,  $R_{\text{equip}}(t)$  is the risk caused by equipment failure, and  $(\alpha, \beta, \gamma)$  is the weight coefficient. Calculating the comprehensive risk can accurately assess the potential risks in the current operation and provide targeted early warning or decision support.

Operational behavior simulation and risk identification are based on precise behavior modeling, real-time risk assessment and multi-dimensional data integration, which effectively improves the operational safety and emergency response capabilities of power grid operators in complex power grid scenarios.

### 3.4 Dynamic Verification and Feedback Mechanism

#### 3.4.1 Dynamic Verification Algorithm

The dynamic verification algorithm verifies every action of the operator in time according to the updated power grid data. The algorithm uses the acquired device status information to compare the planning behavior of the operator with the actual situation and detect possible deviations during the operation. Dispatcher can find potential risks in time before operation to avoid mistakes in actual operation.

Starting from the status information of each device in the power grid, the operation of the power grid can be monitored, and combined with the operator's operating instructions, it can be judged whether it complies with the power grid operation rules. Comparing the ideal state corresponding to the power grid equipment status and the operator's expected behavior, the deviation formula of the operation behavior is expressed as follows:

$$D(t) = \sum_{i=1}^n |S_i(t) - S_i^*(t)| \quad (12)$$

$S_i(t)$  is the actual state of the grid equipment  $i$  at time  $t$ , and  $S_i^*(t)$  is the ideal state. This deviation can effectively evaluate the gap between the operator's current

behavior and the actual state of the grid. Dynamic verification can also combine the mutual influence between devices, consider the coupling effect of power flow, and use the power flow equation to further correct the state deviation.

Considering the complex coupling relationship between various devices in the power grid, power flow calculation is used to dynamically correct the changes in device status. The power flow change can be expressed by the following equation:

$$\Delta P_i = \sum_{j=1}^n X_{ij} \cdot \Delta V_j \quad (13)$$

$\Delta P_i$  represents the change in the power of device  $i$ ,  $X_{ij}$  is the coupling coefficient between devices  $i$  and  $j$ . The dynamic verification algorithm can effectively handle the interaction between grid devices, correct deviations in time, and ensure that the grid state is consistent with the expected operating behavior.

### 3.4.2 Feedback Mechanism

The dynamic verification results provide real-time feedback information for power grid dispatchers. The feedback mechanism can automatically generate operation suggestions based on the verification results to assist dispatchers in making timely and effective decisions. The core of the feedback mechanism is to optimize and adjust the operation behavior based on the real-time verification results.

The verification results of each operation's behavior are analyzed to automatically determine whether the operator's behavior is biased. The feedback mechanism is used to provide corresponding adjustment suggestions to the dispatcher to guide him to correct the operation steps or adjust the strategy; the feedback adjustment process can be expressed by the following formula:

$$\Delta u(t) = -K \cdot D(t) \quad (14)$$

$\Delta u(t)$  is the operation adjustment,  $K$  is the control gain, and  $D(t)$  is the operation behavior deviation. The control gain can calculate the appropriate adjustment amount based on the operation deviation to guide the operator to make timely corrections. The real-time effect of the feedback mechanism allows dispatchers to obtain operation guidance in a timely manner, improving decision-making efficiency and accuracy.

The feedback mechanism has adaptive characteristics. The system can monitor new operating behaviors and re-check them. The feedback of each operation adjustment can provide more references for power grid dispatching, optimize operating procedures, reduce errors, and improve the overall efficiency and safety of power grid operation. Fig. 2 shows the dynamic verification and feedback mechanism process of power grid operation behavior.

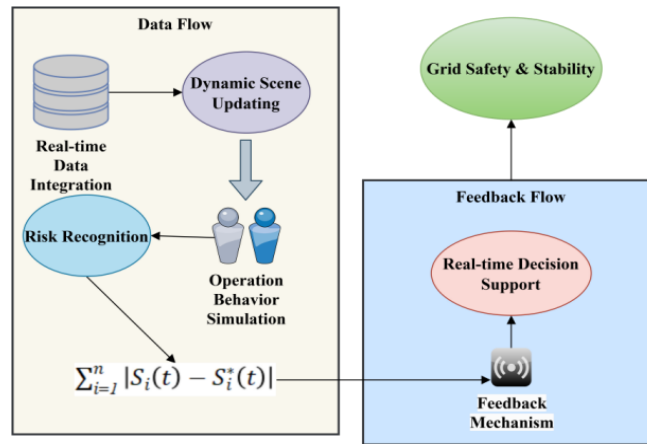


Fig. 2. Dynamic verification and feedback mechanism flow of power grid operation behavior

#### 4. Method Effect Evaluation

##### 4.1 Three-Dimensional Modeling of Power Grid Equipment and Kalman Filter Data Optimization Effect

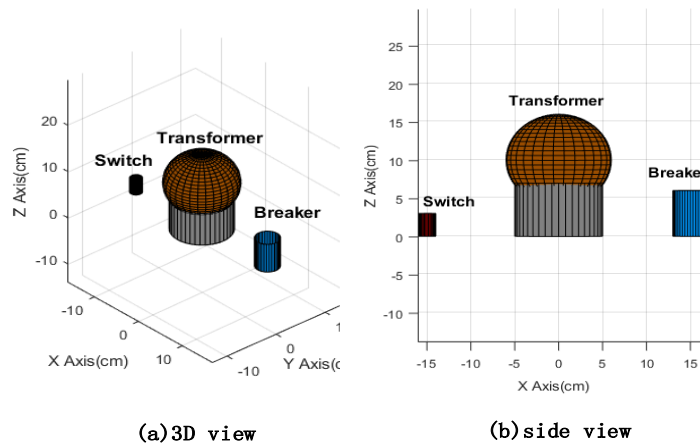


Fig. 3. 3D modeling of power grid equipment

Fig. 3 shows a 3D modeling scene of a transformer, circuit breaker and switch of a power grid equipment. The transformer is modeled using a combination of cylinders and spheres, reflecting its main body and top shape. The cylinder has a radius of 5cm, a height of 7cm, and a top sphere radius of 6cm, reflecting the actual size and structure of the transformer. The circuit breakers and switches are modeled with smaller cylinders, with a radius of 2 cm and a height of 6 cm for the circuit breakers and a radius of 1 cm and a height of 3 cm for the switches, reflecting the size differences of different devices in the power grid. The shape of each device accurately reflects the layout of the actual power grid, which helps to accurately simulate the interaction between devices in the virtual scene. Fig. 3 shows that

through detailed 3D modeling, operators can conduct realistic operation rehearsals in a virtual environment, maintain the accuracy of grid equipment operation, and provide accurate decision support in changing environmental conditions.

Fig. 4 shows the impact of the Kalman filter optimization process on real-time data. Fig. (a) shows the comparison of the raw measurements, the real data and the Kalman filter estimation data. The red curve represents the noisy measurement data, the blue curve represents the real data, and the green curve represents the estimated data after Kalman filter optimization. It can be seen that the real data presents a relatively smooth sinusoidal waveform, representing the actual state of the power grid operation, while the measurement data is affected by the sensor noise and shows obvious fluctuations.

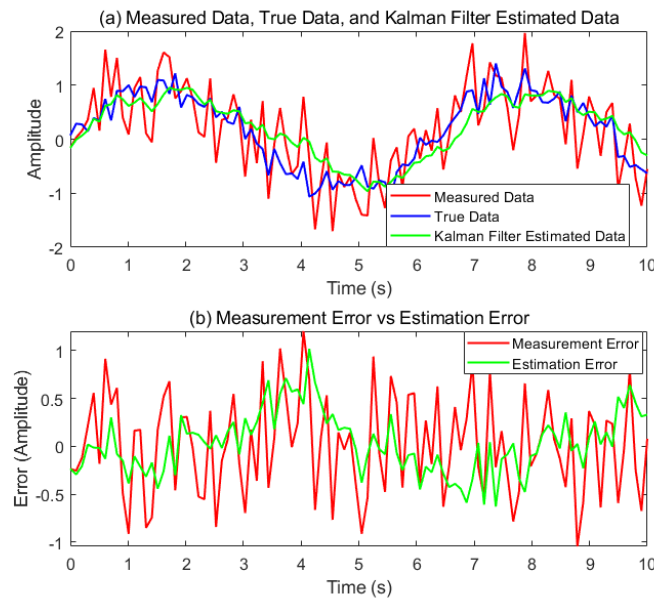


Fig. 4. Kalman filter data optimization

After data prediction and updating, Kalman filtering effectively removes noise, and the estimated data gradually approaches the real data, showing a trend close to the real data. Fig. (b) shows the comparison between the measurement error and the estimation error; the red curve represents the measurement error, showing the difference between the measured data and the real data, and the error fluctuation is large. The green curve is the Kalman filter estimation error, and the estimation error is relatively small, indicating that Kalman filtering can reduce both the noise and the error in the measurement data. Kalman filter can optimize the raw data through dynamic adjustment to provide more reliable data support for monitoring and decision making.

## 4.2 Operation Success Rate and Reaction Time

The experiment was designed using a multi-scenario power grid operation rehearsal platform built using VR technology. The platform simulates a variety of power grid fault operation scenarios. In each virtual scenario, the operator needs to complete a specific power grid operation task, and the operation success rate and reaction time are recorded during the process. The success rate compares the preset task target with the actual completion status, and the proportion of operators who successfully complete the task in each scenario is counted. Reaction time measures the time from the start of a task to the operator making a decision or completing an operation, evaluating their reaction speed. VR technology is compared horizontally with traditional desktop simulation and 2D simulation platforms; the same task scenario is set to record the reaction time and decision accuracy of operators on different platforms. Data collection takes into account factors such as environmental complexity and task difficulty to ensure the effectiveness and representativeness of the experimental results and then evaluate the advantages of VR technology in power grid operation training.

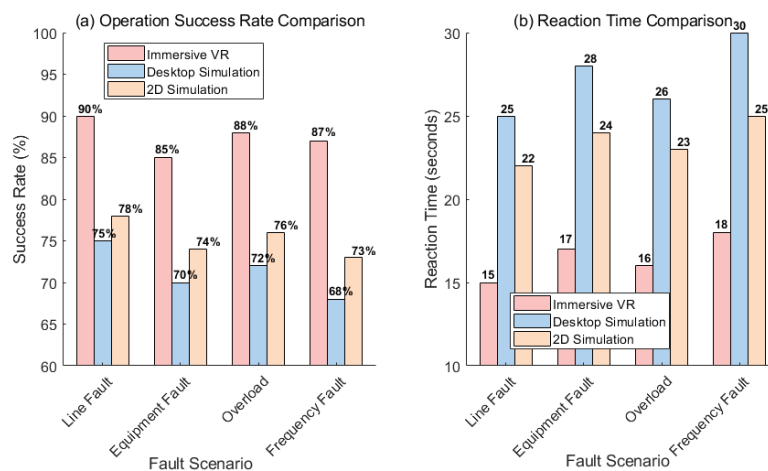


Fig. 5. Comparison of operation success rate and reaction time

Fig. 5 shows the comparison of operation success rate and reaction time of immersive VR technology, traditional desktop simulation platform and 2D simulation platform under four different fault scenarios. In the comparison of operation success rates, the success rate of immersive VR technology is generally higher than that of traditional methods. In the four fault scenarios, VR technology performed well, with success rates of 85% and above. The success rates of desktop simulation and 2D simulation platforms were slightly lower, and under frequency fluctuation faults, the success rates dropped to 68% and 73% respectively. VR technology can better simulate complex power grid environments, improve the decision-making efficiency of operators, and reduce the occurrence of operational

errors. In the comparison of reaction time, the reaction time of VR technology is relatively short, with an average reaction time of 16.5 seconds in four fault scenarios. The reaction time of desktop simulation and 2D simulation platform is longer, more than 20 seconds. VR improves the decision-making efficiency of operators, can quickly respond to complex power grid faults, and provide more timely and effective support for power grid dispatching. These results also fully verify the advantages of immersive VR technology in power grid operation training, which can significantly improve the operation success rate, shorten the reaction time.

### **4.3 Risk Identification Accuracy**

The proposed method integrates real-time positioning data and dynamic environmental variables, monitors the matching between operation behavior and grid status in real time, and identifies potential risks. Using the risk identification accuracy as an indicator, the proposed identification method based on behavior simulation is compared with traditional rule-based risk identification and fuzzy logic-based risk identification to verify the accuracy of risk identification.

Fig. 6 shows the accuracy comparison of three risk identification methods in four power grid failure scenarios. The three methods are risk identification method based on behavior simulation, risk identification method based on rules, and risk identification method based on fuzzy logic. The behavior-based identification method showed the highest accuracy in all scenarios, with an average accuracy of about 90%. The accuracy in the line fault scenario reached 92%, and the accuracy in the load overload fault scenario was 90%. The traditional rule-based risk identification method had a lower accuracy, generally failing to exceed 75%. This difference reflects that the rule-based method has limited recognition accuracy when dealing with complex power grid faults due to the limitations of rules and the inability to adapt to changes in different scenarios. The accuracy of the recognition method based on fuzzy logic is higher than that of the rule-based method, but still lower than that of the behavior simulation-based method. In the equipment failure and frequency fluctuation failure scenarios, the accuracy of the fuzzy logic method is 78% and 77%, indicating that it has certain recognition biases when dealing with some complex situations. The behavioral simulation recognition method improves the risk recognition accuracy of power grid failures and has high practical value when dealing with complex power grid environments and variable fault scenarios.

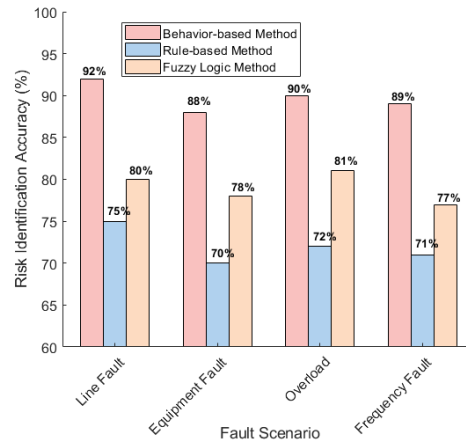


Fig. 6. Comparison of risk identification accuracy

#### 4.4 Dynamic Verification Error and Correction Effect

The dynamic verification error and correction effect evaluation utilizes a VR platform to conduct real-time verification of operating behaviors and continuously monitor the gap between operating behaviors and the actual operating status of the power grid. Error evaluation uses two indicators, MSE and MAE. MSE is used to measure the square difference of the deviation of the operation behavior, which can reflect the overall fluctuation of the error; MAE calculates the sum of the absolute values of the errors and intuitively shows the average degree of the calibration error. During the evaluation, the system collects the operation data of the power grid equipment and the behavior data of the operator in real time, compares the difference between the two, and calculates the corresponding error value. It compares the data before the introduction of the dynamic verification algorithm to evaluate the improvement of the verification error correction effect and analyze the impact of dynamic verification on error correction.

Fig. 7 shows the changes in MAE and MSE in dynamic calibration before and after the introduction of the dynamic calibration algorithm. Over time, both MAE and MSE show a significant downward trend after the introduction of the dynamic calibration algorithm. The dynamic calibration algorithm can effectively reduce the error between the operating behavior and the actual operating state of the power grid. In 60 seconds, after the introduction of the dynamic verification algorithm, MAE and MSE were 0.03 and 0.002 respectively. The decrease in MAE and MSE reflects that the algorithm can effectively reduce the gap between prediction and reality in real-time adjustment of operation behavior. In longer operations, the error converges faster.

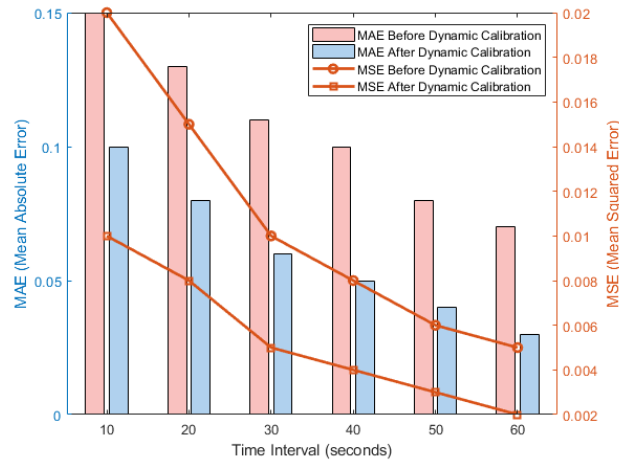


Fig. 7. Comparison of MAE and MSE before and after the introduction of the dynamic calibration algorithm

This data change shows that the dynamic verification mechanism can more accurately correct operator behavior and reduce the risk of error accumulation in long-term system operation. The change in MSE is as obvious as that in MAE. The algorithm's correction of errors not only improves the deviation, but also significantly reduces the error fluctuation. This result suggests that in long-term complex power grid operations, dynamic verification algorithms are of great significance for improving stability and accuracy. The introduction of dynamic verification algorithms can monitor and calibrate operating behaviors in real time, and can also use dynamic adjustment feedback mechanisms to continuously optimize power grid operations, reduce misoperations and potential risks.

## 5. Conclusions

After the verification of a large number of experimental data, this study proves the use effect of multi-scenario preview and dynamic verification method based on VR technology in power grid operation risk identification and dispatching decision. The experimental results show that the highly simulated three-dimensional virtual scene can accurately reproduce the state of power grid equipment, operator behavior and environmental changes, and realize dynamic simulation with high consistency between virtual and real. In various fault scenarios, the system operation success rate reaches 85% or more, the average response time is about 16.5 seconds, and the risk identification accuracy rate reaches about 90%. By integrating real-time positioning data, operation ticket information and dynamic environmental variables, and introducing Kalman filtering and dynamic verification algorithms, data noise and measurement errors are effectively reduced, and a correction effect of MAE of only 0.03 and MSE of 0.002 is achieved within 60 seconds. This innovative combination not only ensures the real-time consistency of operation behavior and

equipment status but also provides data-driven real-time feedback and accurate decision-making support for power grid dispatching. This study has achieved an original breakthrough in the deep integration of VR technology and dynamic verification algorithms, providing a new technical path for improving the safety of power grid operation and the efficiency of emergency response.

### Acknowledgment

This work was supported by the project: Machine-Based Cooperative Control Technology for “Dispatching-Transformation” Operation Safety. Project Number: GDKJXM20230457(030600KC23040008).

### REFERENCES

- [1] Li Y, Yu C, Shahidehpour M, et al. Deep reinforcement learning for smart grid operations: Algorithms, applications, and prospects. *Proceedings of the IEEE*, 2023, 111(9): 1055-1096.
- [2] Khalid H M, Qasaymeh M M, Muyeen S M, et al. WAMS operations in power grids: A track fusion-based mixture density estimation-driven grid resilient approach toward cyberattacks. *IEEE Systems Journal*, 2023, 17(3): 3950-3961.
- [3] Jahangir H, Lakshminarayana S, Maple C, et al. A deep-learning-based solution for securing the power grid against load altering threats by IoT-enabled devices. *IEEE Internet of Things Journal*, 2023, 10(12): 10687-10697.
- [4] Nafees M N, Saxena N, Cardenas A, et al. Smart grid cyber-physical situational awareness of complex operational technology attacks: A review. *ACM Computing Surveys*, 2023, 55(10): 1-36.
- [5] Khaleel M, Abulifa S A, Abulifa A A. Artificial intelligent techniques for identifying the cause of disturbances in the power grid. *Brilliance: Research of Artificial Intelligence*, 2023, 3(1): 19-31.
- [6] Bhadani U. Pillars of power system and security of smart grid. *International journal of innovative research in science engineering and technology*, 2024, 13(13888): 10-15680.
- [7] Ghorpade S J, Sharma R B. A comprehensive review of demand-side management in smart grid operation with electric vehicles. *Electrical Engineering*, 2024, 106(5): 6495-6514.
- [8] Simbolon R, Sihotang W, Sihotang J. Tapping Ocean Potential: Strategies for integrating tidal and wave energy into national power grids. *GEMOY: Green Energy Management and Optimization Yields*, 2024, 1(1): 49-65.
- [9] Li Y, Ding Y, He S, et al. Artificial intelligence-based methods for renewable power system operation. *Nature Reviews Electrical Engineering*, 2024, 1(3): 163-179.
- [10] Peng F Z, Liu C C, Li Y, et al. Envisioning the future renewable and resilient energy grids—a power grid revolution enabled by renewables, energy storage, and energy electronics. *IEEE Journal of Emerging and Selected Topics in Industrial Electronics*, 2023, 5(1): 8-26.
- [11] Wang G, Fu L, Hu Q, et al. Transient synchronization stability of grid-forming converter during grid fault considering transient switched operation mode. *IEEE Transactions on Sustainable Energy*, 2023, 14(3): 1504-1515.
- [12] Pandey U, Pathak A, Kumar A, et al. Applications of artificial intelligence in power system operation, control and planning: a review. *Clean Energy*, 2023, 7(6): 1199-1218.
- [13] Bahrani B, Ravanji M H, Kroposki B, et al. Grid-forming inverter-based resource research landscape: Understanding the key assets for renewable-rich power systems. *IEEE Power and Energy Magazine*, 2024, 22(2): 18-29.
- [14] Yan K, Li G, Zhang R, et al. Frequency control and optimal operation of low-inertia power systems with HVDC and renewable energy: A review. *IEEE Transactions on Power Systems*, 2023, 39(2): 4279-4295.
- [15] Bernet D, Hiller M. A cascaded H-bridge-based multilevel converter with low energy pulsation for high-power grid applications. *IEEE Transactions on Power Electronics*, 2023, 39(2): 2305-2321.
- [16] Rangarajan S S, Raman R, Singh A, et al. DC microgrids: a propitious smart grid paradigm for smart

- cities. *Smart Cities*, 2023, 6(4): 1690-1718.
- [17] Aravena I, Molzahn D K, Zhang S, et al. Recent developments in security-constrained AC optimal power flow: Overview of challenge 1 in the ARPA-E grid optimization competition. *Operations research*, 2023, 71(6): 1997-2014.
- [18] Tavakoli S D, Dozein M G, Lacerda V A, et al. Grid-forming services from hydrogen electrolyzers. *IEEE transactions on sustainable energy*, 2023, 14(4): 2205-2219.
- [19] Shi W, Qu J, Luo K, et al. Grid-integration and operation of High Proportioned new energy. *Strategic Study of Chinese Academy of Engineering*, 2023, 24(6): 52-63.
- [20] Meng Q, Tong X, Hussain S, et al. Enhancing distribution system stability and efficiency through multi-power supply startup optimization for new energy integration. *IET Generation, Transmission & Distribution*, 2024, 18(21): 3487-3500.
- [21] Du W, Tuffner F K, Schneider K P, et al. Modeling of grid-forming and grid-following inverters for dynamic simulation of large-scale distribution systems. *IEEE Transactions on Power Delivery*, 2020, 36(4): 2035-2045.
- [22] Wang S, Duan J, Shi D, et al. A data-driven multi-agent autonomous voltage control framework using deep reinforcement learning. *IEEE Transactions on Power Systems*, 2020, 35(6): 4644-4654.
- [23] Zhao J, Netto M, Huang Z, et al. Roles of dynamic state estimation in power system modeling, monitoring and operation. *IEEE Transactions on Power Systems*, 2020, 36(3): 2462-2472.
- [24] Ajayi A, Oyedele L, Owolabi H, et al. Deep learning models for health and safety risk prediction in power infrastructure projects. *Risk Analysis*, 2020, 40(10): 2019-2039.
- [25] Zafra-Cabeza A, Velarde P, Maestre J M. Multicriteria optimal operation of a microgrid considering risk analysis, renewable resources, and model predictive control. *Optimal Control Applications and Methods*, 2020, 41(1): 94-106.
- [26] Lv Z, Han Y, Singh A K, et al. Trustworthiness in industrial IoT systems based on artificial intelligence. *IEEE Transactions on Industrial Informatics*, 2020, 17(2): 1496-1504.
- [27] Liu J, Miura Y, Bevrani H, et al. A unified modeling method of virtual synchronous generator for multi-operation-mode analyses. *IEEE Journal of Emerging and Selected Topics in Power Electronics*, 2020, 9(2): 2394-2409.
- [28] Chen M, Zhou D, Blaabjerg F. Modelling, implementation, and assessment of virtual synchronous generator in power systems. *Journal of Modern Power Systems and Clean Energy*, 2020, 8(3): 399-411.
- [29] Ambia M N, Meng K, Xiao W, et al. Interactive grid synchronization-based virtual synchronous generator control scheme on weak grid integration. *IEEE Transactions on Smart grid*, 2021, 13(5): 4057-4071.
- [30] Xiong X, Wu C, Blaabjerg F. Effects of virtual resistance on transient stability of virtual synchronous generators under grid voltage sag. *IEEE Transactions on Industrial Electronics*, 2021, 69(5): 4754-4764.
- [31] Awal M A, Husain I. Unified virtual oscillator control for grid-forming and grid-following converters. *IEEE Journal of Emerging and Selected Topics in Power Electronics*, 2020, 9(4): 4573-4586.
- [32] Hou R, Kong Y Q, Cai B, et al. Unstructured big data analysis algorithm and simulation of Internet of Things based on machine learning. *Neural Computing and Applications*, 2020, 32(10): 5399-5407.
- [33] Yap K Y, Sarimuthu C R, Lim J M Y. Artificial intelligence based MPPT techniques for solar power system: A review. *Journal of Modern Power Systems and Clean Energy*, 2020, 8(6): 1043-1059.
- [34] Omitaomu O A, Niu H. Artificial intelligence techniques in smart grid: A survey. *Smart Cities*, 2021, 4(2): 548-568.
- [35] Shivegowda M D, Boonyasopon P, Rangappa S M, et al. A review on computer-aided design and manufacturing processes in design and architecture. *Archives of Computational Methods in Engineering*, 2022, 29(6): 3973-3980.
- [36] Feng F, Na W, Jin J, et al. Artificial neural networks for microwave computer-aided design: The state of the art. *IEEE Transactions on Microwave Theory and Techniques*, 2022, 70(11): 4597-4619.